Applied Geochemistry 100 (2019) 8–21

Contents lists available at ScienceDirect

Applied Geochemistry

journal homepage: www.elsevier.com/locate/apgeochem

Chemical mobility of inorganic elements in stream sediments of a semiarid zone impacted by ancient mine residues

Isidro Montes-Avila[a], Erik Espinosa-Serrano[b], Javier Castro-Larragoitia[a], Isabel Lázaro[a,c], Antonio Cardona[a,*]

[a] Faculty of Engineering, Universidad Autónoma de San Luis Potosí, Dr. Manuel Nava 8, 78290, San Luis Potosí, Mexico
[b] COARA, Carretera Cedral Km 5+600, 78700, Matehuala, San Luis Potosí, Mexico
[c] Institute of Metallurgy, Universidad Autónoma de San Luis Potosí, Sierra Leona 550, 78210, San Luis Potosí, Mexico

ARTICLE INFO

Editorial handling by Prof. M. Kersten

Keywords:
Sediments
Potentially toxic elements
Mine residue

ABSTRACT

Water availability is a worldwide issue, particularly in semiarid zones. Therefore, it is necessary to know the geochemical processes involved in the mobility of contaminant sources to ensure adequate quality for this resource. Some mining areas of México are of economic importance; however, they are also the sources of large quantities of mine residues, such as the site included in this study. As an important aspect of understanding contaminant mobility in sediments and water, a thorough mineralogical characterization is paramount to identify sources and sinks for relevant elements, in this case, potentially toxic elements (PTEs) such as arsenic (As), lead (Pb) and cadmium (Cd); hence, scanning electron microscopy (SEM), X-ray diffraction (XRD) and chemical analysis were used. The total geochemical distribution was established by means of a modified selective sequential extraction procedure. The results showed that sediments constitute an effective attenuation substrate for mobilized PTEs to groundwater. Hence, arsenic and cadmium were stabilized in the sediments and/or the vadose zone, and although Pb and Zn were identified in groundwater with concentrations above the background values, they were below drinking water standards. Sulfate and total hardness concentrations in the groundwater confirmed the impact of acid mine drainage (AMD) infiltration. Considering that similar sites in Mexico are found along the Sierra Madre Oriental, the methodology of this study could be applied to understand the mobility of PTEs in the sediments and waters of semiarid environments.

1. Introduction

The metallurgical mining and smelting industry is considered one of the most contaminating activities in the world (Alloway, 1995; Salomons, 1995) because it involves the release of different quantities of particulate materials, wastewater effluents, atmospheric emissions and acidic effluents (generated by the natural oxidation of sulfides such as pyrite); mining residues can be enriched in elements such as antimony, arsenic, barium, cadmium, lead and zinc. Therefore, these mine wastes could seriously impact water, sediments, soils, atmosphere and biota. To reduce the negative impact of mine wastes on living organisms, it is important to know their geochemical behavior in these environments, which includes the relative mobility in the surroundings. Of major concern are the oldest deposits because they often contain high concentrations of contaminants due to the inefficiency of the ancient metallurgical processes used (Alloway, 1995) and because the materials have been exposed to climatic conditions that favored the oxidation of sulfides and the subsequent release of acidic effluents, which ultimately provoke the dissolution of other minerals present in the deposits. However, some of these minerals act as neutralizers of the acid, for instance, limestone, dolomite, oxides and some silicates. If the neutralizing capacity is overcome, the acid effluent receives the name of acid mine drainage (AMD), and it can flow indefinitely to the surroundings (Alloway, 1995; Salomons, 1995; Dold, 2003), affecting biota, water, soils and sediments. When AMD reacts with the matrixes mentioned, it is generally neutralized, and several secondary phases are generated (i.e., oxides, oxyhydroxides, sulfates and hydroxysulfates). Therefore, AMD is considered a dangerous effluent in mining zones all around the world (Plumlee, 1999; Dold et al., 2009; Lindsay et al., 2015; Lottermoser, 2007; Árcega-Cabrera et al., 2005; Ramos-Arroyo et al., 2004; Razo et al., 2007; Talavera et al., 2006). On the other hand, the acidic effluents can move across the terrain and be incorporated to fluvial systems, where they can be either transported longer distances or associated with the sediments in secondary phases as oxyhydroxides

* Corresponding author.
E-mail address: acardona@uaslp.mx (A. Cardona).

https://doi.org/10.1016/j.apgeochem.2018.11.002
Received 6 April 2018; Received in revised form 2 November 2018; Accepted 3 November 2018
Available online 05 November 2018
0883-2927/

of iron.

Stream sediments have been considered composite samples of the soil and the weathering products of rocks from upstream sites (Plant and Hale, 1994); therefore, they are used as geochemical tracers for the exploration of areas with mineral deposits of economic interest. Erosion processes distribute dissolved and particulate materials from the source to the stream sediments; Salomons (1998) has estimated that more than 99% of the contaminants are stored in the sediments; in addition, sediments are an effective repository for nutrients. For these reasons, sediments are considered a useful tool for geochemical surveys in river basins.

When mining residues reach a fluvial system, several reactions can occur and modify the composition of the mineral phases in the residues to new secondary mineral phases. Given that some toxic elements can attach to secondary phases, it is important to characterize the new geochemical phases and assess the concentrations of toxic elements in the different minerals.

Based on chemical and physical properties such as solubility in solutions with different ionic force, pH, and reduction-oxidation and complex formation potentials, several schemes of chemical fractionation have been proposed and employed to identify and quantify toxic element concentrations present in specific phases (Tessier et al., 1979; Dold, 2003; Hudson-Edwards et al., 2005; Shang and Zelazny, 2008; Espinosa et al., 2009; Ribeiro de Souza et al., 2016) Then, each fraction or extract corresponds to the elements associated with the “water/acid soluble”, “exchangeable”, “reducible”, “oxidizable” and “residual” fractions present in the analyzed sample (Ure and Davidson, 2002). These methodologies are relatively fast, easy and inexpensive and can generate basic information to continue the investigation with more specialized (sophisticated) methodologies such as scanning electronic microscopy (SEM), Raman spectroscopy and techniques related to synchrotron radiation such as Extended X-Ray Absorption Fine Structure (EXAFS) (Brown et al., 2006).

A semiarid region is considered (Burdon, 1998) a transition zone between the arid deserts and the subhumid belts, where the controlling factors are clearly low annual precipitation (mainly in episodic events of high intensity), extreme temperatures and evaporation. Attention has been focused in several areas around the world, for example, the Cartagena-La Unión mining District in Spain (Navarro et al., 2008; García Lorenzo et al., 2012), Arizona in the United States (Hayes et al., 2012) and the north-central zone in Chile (Espejo et al., 2012). In México, the semiarid zone is located in the central part of the country where there are several mining zones of great importance with activities developed over centuries, and in fact, there are some reports about the contamination of different magnitudes that has occurred there (Castro-Larragoitia et al., 1997; Razo et al., 2004; Gómez-Álvarez et al., 2011).

In Mexico, there are some examples of studies of geochemical fractionation carried out in mining zones affected by mine wastes in semiarid regions, such as the following: Zimapán in Hidalgo state (Espinosa et al., 2009), the Sonora desert (Gómez-Álvarez et al., 2011), and Xichú in Guanajuato state (Carrillo-Chávez et al., 2014). Due to a long mining history, many semiarid zones of northern México present large deposits of historical mine wastes (Carrillo-Chavez et al., 2003; Razo et al., 2007; Castro-Larragoitia et al., 1997, 2013) that deserve attention because they have not been protected against weathering agents (as a result, they have been dispersed to different distances) and because they contain high concentrations of toxic elements, often involving the generation of acid mine drainage (AMD). These residues have been deposited on the banks of streams and rivers where the dispersivity is significantly increased (Smith and Huyck, 1999).

Several studies have been conducted in this area to describe its environmental history (Martínez Chavez, 2012), to evaluate the physiology of the vegetal species that grow in impacted mining sites (Rodríguez Torres, 2013), to characterize the deposits of ancient mine wastes and to evaluate their impact on soil (Razo et al., 2007; Rodríguez-Rodríguez, 2011; Vázquez, 2012).

Current research about the environmental behavior of inorganic contaminants has been mainly focused on their hazardous nature, the threat they represent for living organisms and their negative impact on the quality of water and soil resources. Arsenic, barium, cadmium, copper, chromium, lead, nickel and zinc are inorganic contaminants of particular relevance due to their known toxicity and, in some cases, poisonous and carcinogenic nature. In this regard, special attention has been given to the dispersion of these elements from mining areas around the world.

The contaminants’ potential mobility from mining and mineral processing activities depends on the (1) mineral source; (2) abundance of the mineral; (3) rates and mechanisms of mineral dissolution and precipitation relative to the flow rate of water; and (4) water (and air) flow paths because concentrations of constituents in natural waters depend to a large extent on the rate of dissolution relative to the flow rate of the water (Berner, 1978; Maher, 2010).

In this work, the distribution of potentially toxic elements (PTEs) in the different mineral phases associated with ancient residues and sediments has been evaluated by means of applying a modified sequential extraction methodology combined with mineralogical characterization. This research is important because the mobility of the evaluated elements poses a threat to the environment, particularly to sediments and water quality in zones where the water is scarce, as is the case in semiarid climatic zones.

2. Study site

2.1. Location

The study area is located in the eastern portion of the San Luis Potosí drainage basin, approximately 19.5 km from San Luis Potosí City (Fig. 1) and about 420 km north of Mexico City. This district has an ancient mining history that began in the late XVI century, and there has been intermittent activity throughout this time associated with the exploitation of lead-silver and gold deposits.

2.2. Geology

The geological setting of the study area (Labarthe, 1982; Lopez-Doncel, 2003), as presented in Fig. 1, is composed of outcrops of Lower Cretaceous sedimentary rocks (limestones and shales) of the La Peña, Indidura and Cuesta del Cura formations, unconformably overlain by continental sediments and volcanic rocks (Eocene-Oligocene) with variable compositions from andesite to rhyolite. Basin-fill sediments overlie volcanic rocks in the plain of the drainage basin, and Quaternary alluvial deposits include sediments along intermittent streams.

The economic mineralization is associated with a dioritic intrusive of Tertiary age with porphyritic alteration and tabular form from 15 to 500 m thick, intruding along fractures and stratification planes in the Cuesta del Cura Formation and producing replacement ore bodies; some cavity fillings that form layers and chimneys with disseminated mineralization are present as stockworks composed of calcite veinlet networks with iron oxides (goethite) and deep sulfide zones (pyrite, sphalerite, tetrahedrite, arsenopyrite, chalcopyrite and acanthite).

2.3. Hydrology

The study area has semiarid conditions (390 mm/annum for the 1951–2010 period; SMN, 2015), is drained by the San Pedro stream (Fig. 1), and is located in the San Luis Potosi drainage basin; the stream has an area of approximately 172 km^2 with a dendritic pattern and an intermittent main stream length of 10.9 km. There is a small reservoir ($< 1000\ m^3$) in the highlands of the basin. The mobility and dispersion of the sediments in the basin are usually produced by runoff from high-intensity summer storms.

The drainage basin of San Luis Potosí includes two aquifer units: i) a

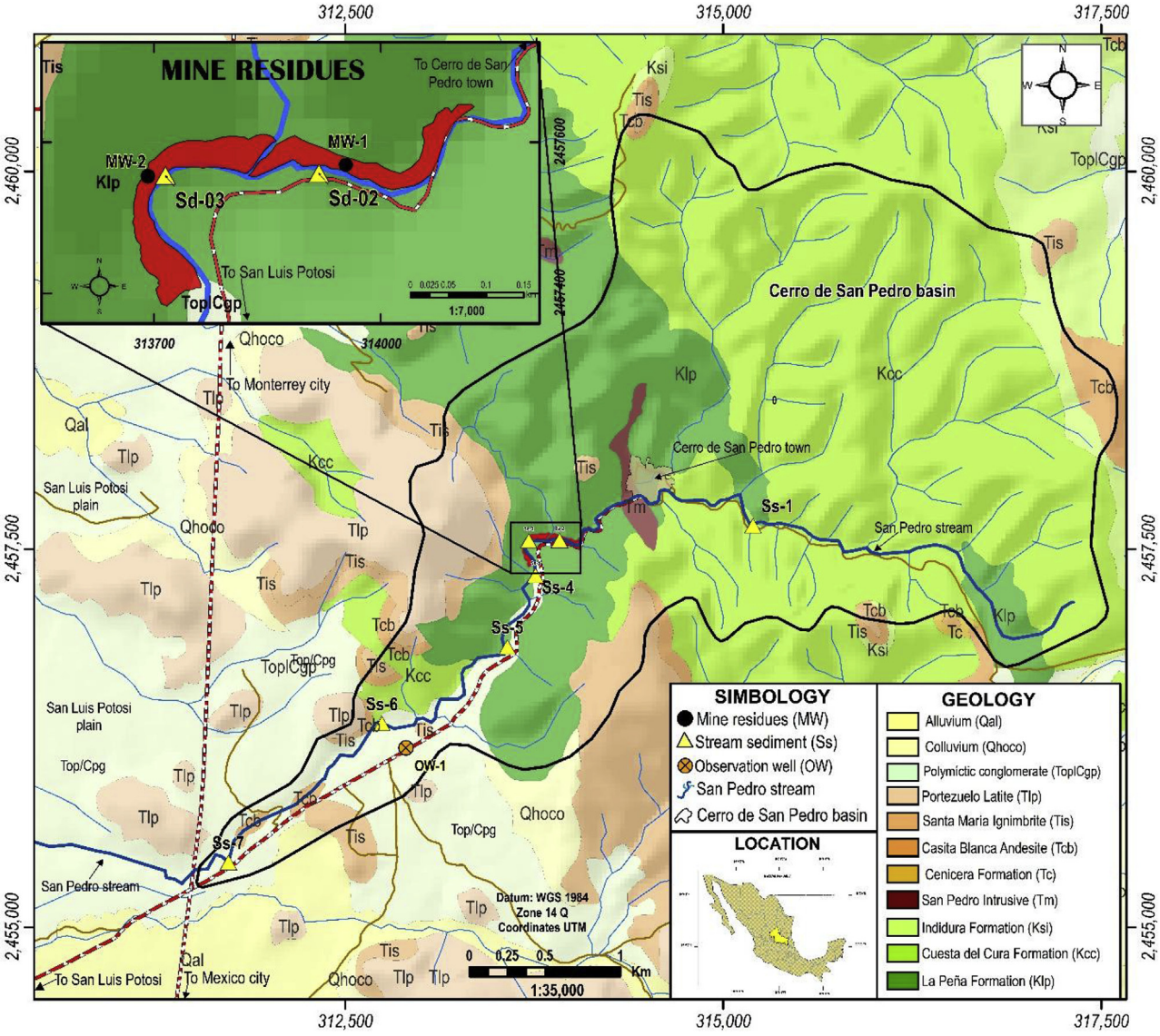

Fig. 1. Geological setting and sampling sites in the study area.

shallow (perched) aquifer and ii) a deep aquifer. The shallow aquifer unit has an irregular distribution: it contains local groundwater flows in Quaternary alluvium and basin fill (sand and silt with variable amounts of clay) and has a maximum thickness of approximately 50 m. Intermediate and regional groundwater flow systems circulate in the basin-fill sediments and fractured volcanic rocks (deep aquifer unit), which has a regional extension beyond the surface drainage basin boundaries. Cretaceous limestone and calcareous mudstone and the post-Mesozoic granodiorite intrusion form the hydrogeological basement (Cardona et al., 2018).

2.4. Mine residue

Due to the high economic value of the deposits previously mentioned, mining activities have been developed for over 400 years, but the highest production of mineral concentrates was observed in the middle of the last century, with the subsequent generation of approximately 150,000 ton of gangue mine wastes enriched in sulfides (Razo et al., 2007) with heterogeneous granulometry and composition. These mine wastes accumulated on the banks of the San Pedro stream (Fig. 1). Vázquez (2012) classified this deposit into two parts: i) the east one is semiconfined by the wall rock and comprises materials with high quantities of oxidized minerals and low sulfide content and surficial spots of secondary minerals (i.e., elemental sulfur and sulfates of calcium and of zinc), and ii) the west unconfined zone is composed mainly of fine particles with a high content of sulfide minerals. Currently, the slope of the deposit has a hard cover of secondary oxides-oxyhydroxides of iron. The mineralogical and textural differences are related to their origin during different stages of the mining process. Climatic conditions have induced pyrite oxidation and the consequent generation of AMD. As result, the stream has three main inputs of contaminants from the mine residues: residues in particulate form, acid effluents (AMD) and secondary mineral phases (oxides, sulfates, hydroxides) (Schaider et al., 2014).

3. Methodology

This section describes the most important aspects related to the field work and the experimental methodology followed in this research.

3.1. Sampling

Sampling site selection involved a field survey to identify the mine residue locations and characteristics, drainage pattern, accessibility,

Table 1
Quality control information.

Element	LOD (mgL^{-1})	LLOQ (mgL^{-1})	HLQ (mgL^{-1})	MRC 2710A Certified ($mgkg^{-1}$)	MRC 2710A Measured ($mgkg^{-1}$)	Recovery (%)
As	0.0207	0.0621	102	1540	1566	102
Cd	0.0022	0.0066	5	12	22	117
Zn	0.0205	0.0615	247	4180	4194	100
Pb	0.0817	0.2450	26	5520	6112	111
Cu	0.0196	0.0587	26	3420	3185	93
Fe	0.0205	0.0615	246	43200	43836	101
Ca	0.0675	0.2024	249	9640	9586	99
S	0.3869	1.1606	11	N. A.	N. A.	N. A.
Mn	0.0214	0.0643	26	2140	2099	98

LOD = Limit of Detection of the Method calculated (LLOQ/3). LLOQ = Lower Limit of Quantification. HLQ = Higher Limit of Quantification. N. A. = Not apply.

slopes and geology. One sampling site was selected in the small reservoir upstream from the main residue location. Other sampling sites were selected along the stream adjacent to the mine residues. Additionally, sampling sites downstream were selected to fully understand the sediment dispersion and the mobility of PTEs.

Sediment samples were collected in March 2014 using a steel shovel in the top 5 cm, making a shallow sampling ditch along the stream bed traverse. The sampling points for sediments (Fig. 1) were located along the streambed, the first in the upper part of the basin, 6 km from the most important mine waste deposits and without evidence of anthropogenic alteration; two sites were located in front of the residue deposit; and 4 sites were located downstream from the residues (Table 1) to evaluate the transport and accumulation of contaminated sediments along the stream.

To compare and to estimate the influence on the sediments, two samples of mine residues were taken. The mine residue samples were collected along the slope after the removal of the coarse and weathered (cemented) surficial materials. All the samples were sieved with stainless steel 2 mm mesh and quartering *in situ*. Approximately 1.0 kg of fine materials were collected in clean plastic bags.

Groundwater samples from an observation well (OW-1, 81 m deep) located in the San Pedro stream and a production well (PW-1, 600 m deep) were taken during a three years period (2013–2016) using a bladder pump and pumping equipment, respectively. Field measurements of temperature, electrical conductivity (EC), pH, Eh (Pt electrode) and dissolved oxygen (DO) were carried out using a closed flow-through isolation cell; calibrations of the portable field equipment were made at each site for pH (4.0 and 7.0 buffer solutions) and DO measurements, and the appropriate performances of the Pt electrode and the EC electrode were controlled with a Zobell solution (3×10^{-3} M potassium ferrocyanide and 3×10^{-3} M potassium ferricyanide in 0.1M KCl) and a calibration solution, respectively. Acid-base titration (Gran method) was used for total alkalinity determination. At each site, different aliquots were collected for laboratory analyses. For major and trace element analyses, the samples were filtered (0.45 µm) and collected in double acid-washed, low-density polyethylene bottles; the samples for analyses of cations and trace elements were stabilized with the addition of 1% ultrapure HNO_3 to improve the stabilization of elements, and samples for NO_3 determinations were acidified to pH of 2 with H_2SO_4. The samples for anion analysis were not acidified.

3.2. Sampling conditioning and acid digestion of sediments and mine residue

The samples were dried at room temperature for five days and then pulverized in a mechanical mortar grinder (Retsch) to a final particle size of 10 µm. Approximately 0.2 g of each dry sample with 2.0 mL of hydrofluoric acid (HF) and 3.0 mL of nitric acid (ACS quality) was added to a Teflon vessel and digested in a microwave reaction system model MARS 6 following the EPA method 3052 (USEPA, 1996; CEM, 2015a). Then, the HF in the digested samples was neutralized with 5 mL of an aqueous solution of boric acid (4% v/v) as described by CEM (2015b). Quality control was achieved by laboratory blank duplicates and reference certified material (MRC 2710A).

3.3. Groundwater analysis

Analyses for major (Cl^-, SO_4^{2-}, Na^+, Ca^{+2}, Mg^{+2}) and minor (K^+, F^-, NO_3^-) ions were completed following the standard protocols described in Eaton et al. (2005). Chloride was analyzed by titration with $AgNO_3$; SO_4^{2-}, by a gravimetric method; and NO_3^-, by automated colorimetry; F^- concentrations were verified using the SPADNS method. Major (Ca^{2+}, Mg^{2+} and Na^+) and some minor (K^+ and Sr^{2+}) cations and Si were analyzed by an inductively coupled plasma optical emission spectrometer (ICP-OES), Thermo Scientific model ICAP 7400); trace elements, by an inductively coupled plasma mass spectrometer (ICP-MS) Thermo Scientific model ICAP 7400, Perkin Elmer ELAN 9000. The accuracy of ICP-OES and ICP-MS analyses was controlled using duplicate analyses and appropriate laboratory standards and checked during each batch using international reference standards, including NIST-1640 and SLRS-4. The results of groundwater chemistry were within 5% ionic balance.

3.4. Mineralogical characterization

The mineralogy of representative matrix samples was analyzed using an X-ray diffractometer (XRD) Bruker model D8-Advance; the diffraction data were collected from 10 to 90°, 2Θ (Cu radiation with a wavelength of 1.5405 Å); the method has a detection limit of approximately 5 wt %. To complement these characterizations, samples were investigated using a scanning electron microscope (SEM) JEOL model JSM-6610 LV with a backscattering electron detector (BSE) and an energy dispersive detector (EDS) for the elemental analysis, as well as the use of a multielemental microanalysis tool by means of scanning on specific areas or particles of the samples of interest.

3.5. Total chemical characterization

The total concentrations were determined using and ICP-OES Thermo Scientific model ICAP 7400 Duo calibrated with multi-elemental standards prepared at various concentrations with high-purity certified stock solutions. All the calibration curves were considered with $r^2 \geq 0.99$. The elements were measured in two modes: axial (for lower concentrations, e.g., < 1.0 ppm) and radial (for higher concentrations) with different wavelengths as shown in Table 1.

The quality control criterion to accept the recoveries was ± 20% difference from the certified value as recommended by international organizations (USEPA, 2014). The standard reference material used was Montana I soil 2710a (MRC 2710A), Highly Elevated Trace Element Concentrations, from NIST. The recovery values are presented in Table 1.

The pH of all samples was measured following EPA method 9045D (USEPA, 2004); a potentiometer Horiba model EX-20 was used and

Table 2
Selective sequential extraction tests scheme (modified from Dold, 2003).

Fraction	Reactant or solution	Conditions	Geochemical fraction
(F1) Elements soluble in simulated meteoric water	Deionized water, pH = 5.5	Shake for 24 h at room temperature (RT)	Secondary salts soluble in water
(F2) Elements exchangeables and associated with carbonates and sulphates	1 M ammonium acetate, pH = 4.5 (with acetic acid)	Shake for 2 h at RT	Exchangeable elements, carbonates, sulphates
(F3) Elements associated with iron oxy-hydroxides	0.2 M ammonium oxalate, pH = 3 (adjust with oxalic acid or nitric acid)	Shake for 2 h in darkness at RT	Secondary and amorphous oxy-hydroxides of iron
(F4) Elements associated with iron oxides	0.2 M ammonium oxalate, pH = 3 (adjust with oxalic acid or nitric acid)	Keep the mixtures in water bath at 80 °C for 2 h with occasional shake	Primary and secondary crystalline oxides of iron
(F5) Elements associated with organic matter and sulphides	35% hydrogen peroxide, adjusted at pH = 2.0 with nitric acid	Keep the mixtures reacting all night at RT, then keep in water bath at 80 °C for 2 h with occasional shake	Organic matter and sulphides
(F6) Residual	Concentrated nitric and hydrofluoric acid	Microwave-assisted digestion (USEPA method 3052)	Mainly refractory and primary minerals like silicates, quartz

calibrated with buffer solutions at pH 4.0, 7.0 and 9.0.

3.6. Selective sequential extraction tests

The geochemical fractionation of the investigated materials was determined using a modified scheme of selective sequential extraction (SSE) described by Dold (2003) as sequence B, which was developed for copper sulfide mine residues. The procedure is presented in Table 2. Thus, given that typical runoff produced by a high-intensity storm lasts for several hours (at least 12–24), the F1 was modified to resemble these conditions. Steps 5 and 6 from Dold (2003) were merged as F5 (Table 2) because the copper sulfide content is lower than 2%. In every SSE test, the mixture was centrifuged at 3500 rpm for 10 min using an Eppendorf centrifuge model 5810r. The supernatant was transferred to 50 mL polypropylene vessels (centrifuge tubes), acidified when required, and filled to a volume of 30–50 mL with deionized water (type A, ≥18 MΩ). All the analytical reagents and acids utilized were ACS grade or higher; the acids were previously distilled in a subboiling Savillex system. All the samples were treated in duplicate, and the average values are reported.

4. Results and discussion

4.1. Sampling

The sampling points for sediments (Fig. 1) were located on the streambed, the first in the upper part of the basin, 1.3 km from the most important mine residue deposits and without evidence of anthropogenic alteration; two sites were located in front of the residue deposits; and four sites were located downstream from the residues (Table 3) to evaluate the transport and accumulation of contaminated sediments along the stream. To compare and to estimate the influence over the sediments, two samples of mine residues were taken.

4.2. Mineralogy characterization

The results of XRD and SEM analysis are presented in Tables 4 and 5, respectively. The f allowed the characterization of phases present at contents higher than 5 wt%. Given that secondary phases constitute solubility controls and given the detection limit of XRD, some varieties of jarosite were better identified by means of SEM. In addition, SEM allowed the identification of amorphous phases such as copiapite and iron oxides, which are known as adsorption sites for arsenic (Dold and Fontboté, 2001).

It is important to note that the surficial mine residues present important levels of oxidation and low pH values; samples MW-1 and MW-2 come from the mineralized intrusive, and the sulfides present in the materials are oxidized, suggesting that they have low attenuation capacity, as reported elsewhere (Razo et al., 2007).

Sulfide oxidation in presence of oxygen and water (reactions 1–3) or of ferric ions as oxidants (reaction 4) can generate different numbers of moles of acid. When the acidity increases, different mineral phases are dissolved; then, the concentration of ions can reach the supersaturation level, and at this point, some minerals can precipitate as iron oxy-hydroxides and jarosite (reaction 5) at pH values of approximately 2–3. If the acidity generated is neutralized with calcite in the first instance, several reaction products are formed, such as gypsum (equation (6)) and other metallic sulfates (Plumlee, 1999; Cornell and Schwertmann, 2003; Zhu et al., 2012).

$$FeS_{2\,(s)} + 3.5O_{2\,(aq)} + H_2O_{(l)} \rightarrow Fe^{2+}_{(aq)} + 2SO^{2-}_{4\,(aq)} + 2H^{+}_{(aq)} \quad (1)$$

$$ZnS_{(s)} + 2O_{2\,(aq)} \rightarrow Zn^{2+}_{(aq)} + SO^{2-}_{4\,(aq)} \quad (2)$$

$$PbS_{(s)} + 2O_{2\,(aq)} \rightarrow Pb^{2+}_{(aq)} + SO^{2-}_{4\,(aq)} \quad (3)$$

$$FeS_{2\,(s)} + 14Fe^{3+}_{(aq)} + 8H_2O_{(l)} \rightarrow 15Fe^{2+}_{(aq)} + 2SO^{2-}_{4\,(aq)} + 16H^{+}_{(aq)} \quad (4)$$

$$3Fe^{3+}_{(aq)} + H_3O^{+} + 2SO^{2-}_{4\,(aq)} + 6H_2O_{(l)} \rightarrow (H_3O^{+})Fe_3(SO_4)_2(OH)_{6\,(S)} + 6H^{+}_{(aq)} \quad (5)$$

$$CaCO_{3(s)} + H_2SO_{4(aq)} + H_2O_{(l)} \rightarrow CaSO_4{\cdot}2H_2O_{(s)} + CO_{2\,(g)} \quad (6)$$

Thus, gypsum and a lesser proportion of jarosite appear as predominant secondary phases (> 5.0 wt%) in the sediments and residues associated with the deposits and the presence of AMD. The jarosite is considered a mineral phase that consumes acid when it is precipitated. Gypsum and other salts such as iron sulfates and oxyhydroxides fill intergranular pores and cement the residues below the oxidation zone; the material consolidated is called “hardpan”, and it controls the sulfide oxidation process and AMD generation (Lottermoser, 2007).

Although calcite is a ubiquitous mineral in the study area (it proceeds from the Cuesta del Cura and La Peña formations), it is absent from sediment sample Ss-3 because in this material, the acidity generated by the oxidation of sulfides has consumed this mineral, reducing it to concentrations lower than the detection limit of the XRD instrument employed to characterize the samples. This condition maintains a high mobility of several elements, as shown in the next sections.

4.3. Chemical characterization of the mine residues and surficial sediments along the stream

The total elemental concentrations obtained for sediments and mine residues are presented in Table 6, and the values have standard deviations lower than ± 20%.

The results of the chemical characterization of the mine residues are similar to those obtained by Vázquez (2012) in samples from the same mine residues (Table 7); according to this author, the high concentrations of lead are unusual for a mine residue or a sterile mineral, but XRD

Table 3
General observations of the sites and samples collected.

Sample	Observations of the site and sample (Ss = sediment, MW = mine residue or residue) Coordinates in UTM, datum WGS 85
Ss-1	The sediments were collected upstream from a small dam. The sediments collected presented a dark brown color because of decomposing organic material (humus) that was abundant. This point was located approximately 1.5 km upstream from the deposits of wastes and was considered not impacted by mining activities. Location: 313918 N, 2457560 W and 2047 m.a.s.l.
Ss-2	Sample collected near site MW-1; the materials were mainly gray fine particles associated with surface agglomerated material (crusts) with some fractures due to the natural desiccation of sediments. Additionally, some small red-orange ponds of almost dried acid drainage were observed. The streambed was approximately 4–5 m wide. Location: 313710 N, 2457542 W and 2001 m.a.s.l.
Ss-3	Sample of sediments located near sample site MW-2, where the bed of the stream increased in size and the site conditions favored the accumulation of fine materials (fine sands, clays and silts). These materials were wetted, and some small ponds of acidic drainage were observed. Location: 313762 N, 2457318 W and 1994 m.a.s.l.
Ss-4	The sediments were collected 100 m downstream from the waste deposits where the streambed was approximately 3 m wide. The sediment in the riverbank was composed of boulders, cobbles, gravel, and in the center, fine materials (sand and clays) predominated. The color of the shallow sediments was reddish, and the color was ochre at depth. Location: 313634 N, 2457032 W and 1986 m.a.s.l.
Ss-5	The streambed was approximately 10 m wide with abundant deposit of fine materials. The sediments were wet, and the particle were predominantly sand, clays and silts of gray color, partially consolidated; some boulders were removed manually. The distance to the mine residues was approx. 500 m upstream. Location: 313573 N, 2456855 W and 1973 m.a.s.l.
Ss-6	This point was located 2.3 km downstream from the mine residues with some terrain dedicated to agricultural activities. The materials in the riversides were predominantly cobbles and boulders; in the center was a sand bar with abundant fine particles. The streambed was 2 m below the soil (terrain) level and was approximately 10 m wide. Location: 312744 N, 2456348 W and 1933 m.a.s.l.
Ss-7	The streambed was approximately 6.0 m wide and composed of pebbles, fine sands, clays and silts (some slags were also found scattered in the bed). The surficial sediments collected were gray in color and dry, and the deeper materials were predominantly pebbles and cobbles. This point was 3.17 km downstream from the mine residues. Location: 311729 N, 2455429 W and 1914 m.a.s.l.
MW-1	Sample was collected in a shallow dig made along the slope of a deposit of unconfined mine wastes. The material was heterogeneous in texture and color (from white to gray, ochre and yellow); at the surface, there was a crust of ochre oxides that was removed; only gray-greenish materials with small particle size (< 2.0 mm of diameter) were collected. Location: 313729 N, 2457589 W and 2001 m.a.s.l.
MW-2	The wastes in this deposit were semiconfined and had heterogeneous composition. The sample was collected in the same manner as sample MW-1. Location: 313946 N, 2457571 W and 2013 m.a.s.l.

Table 4
Mineral phases identified (✓) by X-ray diffraction analysis.

Minerals identified	Sample					
	Mine residues		Sediments			
	MW-1	MW-2	Ss-1	Ss-2	Ss-3	Ss-4
Albite [$K_{0.2}Na_{0.8}AlSi_3O_8$]	–	–	✓	–	–	–
Biotite [K Fe Mg_2 (Al Si_3O_{10}) $(OH)_2$]	–	–	–	–	✓	–
Calcic montmorillonite [(Ca, $Na)_{0.3}Al_2(Si, Al)_4$ $O_{10}(OH)_2.XH_2O$]	–	–	✓	✓	–	–
Calcite [$CaCO_3$]	–	–	✓	✓	–	✓
Chalcopyrite [$CuFeS_2$]	–	–	–	–	✓	–
Chloritoid [$(Fe, Mg)_2Al_4Si_2O_{10}$ $(OH)_4$]	–	–	✓	–	–	–
Gypsum [$CaSO_4$. $2H_2O$]	✓	✓	–	–	✓	✓
Halloysite [Al_2 Si_2 O_5 $(OH)_4$]	–	–	–	✓	–	–
Hydronian jarosite [(K,H_3O) $Fe_3(SO_4)_2(OH)_6$]	✓	✓	–	–	✓	–
Kaolinite [Al_2 Si_2 O_5 $(OH)_4$]	✓	–	–	✓	–	✓
Muscovite [K Al_2 (Si, Al)$_4$ O_{10} $(OH)_2$]	✓	–	–	✓	–	✓
Nacrite [$Al_2Si_2O_5(OH)_4$]		✓		✓	–	–
Quartz [SiO_2]	✓	✓	✓	✓	✓	✓

(Table 4) and SEM (Table 5) characterization showed that lead is related to the presence of phases of galena, plumbojarosite, coronadite and cerussite.

The results of the total chemical analysis of the mine residues indicate that the concentrations of sulfur and lead are the highest, reflecting the abundance of sulfides and particularly galena. From the data obtained, it can be observed that the concentrations of arsenic, iron, lead and sulfur are the main indicators of the influence of the mine residues on the sediments, in particular sediment sample Ss-3, which is the sample with major input of these elements from the residues. Conservative mixing calculations in a two end-member system indicate that Ss-3 has approximately 70% of the mine residue end member for sulfur, As and Fe (Fig. 2). Meanwhile, calculations involving lead and arsenic show lower values, suggesting that lead has mobilized from deeper zones of the sediment. Downstream sediments and Ss-2 maintain the same contribution from the mine residue end members (ca. 4–19%), indicating that the conditions are not favorable for lead mobilization.

In general, the results are comparable with those obtained by Hudson-Edwards et al. (2005) in the top sediments of ephemeral floodplain pools in Spanish rivers impacted by a flood of mining wastes in 1998; further, in contrast, the pH remained constant (nearly 7.0) in the sediments collected in this research. Although small ponds of AMD were found in the streambed immediately after precipitation events (in Ss-2 and Ss-3), this neutral condition is maintained due to the natural abundance of calcite in the area. For example, the presence of carbonate minerals (calcite, dolomite and siderite) has been considered to promote natural neutralization of AMD in zones impacted by the oxidation processes of sulfides (Al et al., 2000; Dold et al., 2009; Espinosa et al., 2009) as described in reaction 6.

Furthermore, the concentrations of calcium have a different behavior compared with those of sulfur: the highest content of sulfur (mean of 92686 $mgkg^{-1}$) was quantified in mine wastes and in the sediments collected in front of them. Downstream, the concentrations decrease gradually in the sediments; then, the contents of both elements allowed differentiation of the sediment samples impacted by tailings and those enriched naturally in limestone mainly downstream of the deposits of mine residue (Fig. 3).

The correlation analysis of the elemental concentrations and pH measured in the sediment samples (Table 8) show that pH only influences calcium behavior, as this element is related to the predominant lithology of the area. From the same correlation analysis, some clusters of elements such as As—Cd—Fe—Pb—S—Zn are identified, given that they are present in the minerals of economic value processed in the mining district (COREMI, 1996).

4.4. Downstream distribution of elements

Sample Ss-1 collected in the upper part of the basin represents non-impacted sediments with the lowest measured concentrations of As, Cd, Cu, Pb and Zn (Table 4), which seem to represent the natural concentrations in this region. In Fig. 3, distribution graphs of the elemental concentrations registered downstream are presented. Mine residues have higher concentrations of iron and sulfur than of calcium, derived from their pyrites, oxides, gypsum and limestone content.

As illustrated in Fig. 3, the calcium concentration behaves

Table 5
Mineral phases identified (✓) by SEM analysis.

Mineral phases				Residue		Sediments			
Source	Class	Name	Chemical formula	MW-1	MW-2	Ss-2	Ss-3	Ss-4	Ss-5
Primary	Sulfides	Pyrite	FeS_2	✓	✓	✓	✓	✓	✓
		Galena	PbS	✓	✓	–	✓	✓	✓
		Sphalerite	ZnS	–	✓	–	–	✓	✓
		Arsenopyrite	FeAsS	–	–	–	–	✓	–
		Galena argentiferous	AgPbS	✓	–	–	–	–	–
	Silicates	Quartz	SiO_2	✓	✓	✓	✓	✓	✓
	Carbonates	Calcite	$CaCO_3$	–	–	✓	✓	✓	✓
Secondary	Sulfates	Gypsum	$CaSO_4.2H_2O$	✓	✓	–	✓	–	–
		Melanterite	$FeSO_4$	✓	–	–	✓	–	–
		Anglesite	$PbSO_4$	✓	–	–	✓	–	✓
		Jarosite	$KFe_3^{3+}(SO_4)_2\ (OH)_6$	–	–	–	–	✓	–
		Plumbojarosite	$Pb_{0.5}Fe_3^{3+}(SO_4)_2(OH)_6$	✓	✓	–	✓	–	–
		Hydroniumjarosite	$K_{0.84}(H_3O)_{0.16})Fe_{2.73}(SO_4)2\ ((OH)_{5.19}(H_2O)_{0.81}$	–	✓	–	–	–	–
		Natrojarosite	$NaFe_3(SO_4)_2(OH)_6$	–	✓	–	–	–	–
		Copiapite	$Fe^{2+}Fe_4^{3+}(SO_4)_6(OH)_2{\cdot}20H_2O$	–	✓	–	–	–	–
		Zincopiapite	$ZnFe_4(SO_4)_6(OH)_2.18H_2O$	✓	✓	–	–	–	–
		Aluminumcopiapite	$(Mg,Al)\ (Fe^{3+},\ Al)_4(SO_4)_6(OH)_2{-}20H_2O$	✓	✓	–	–	–	–
		Zincosite	$ZnSO_4$	–	✓	–	–	✓	✓
		Barite	$BaSO_4$	✓	✓	–	–	✓	✓
	Oxides	Coronadite	$Pb(Mn_6^{4+}Mn_2^{3+})O_{16}$	–	–	✓	✓	✓	✓
		Arsenolite	As_2O_3	–	–	–	✓	–	–
	Carbonates	Cerussite	$PbCO_3$	–	–	✓	✓	✓	✓
	Hydroxides	Ferrihydrite	$Fe_5HO_8{\cdot}4H_2O$	✓	–	–	–	–	–
	Elementary	Native sulfur	S	–	✓	–	–	–	–
	Chlorides	Mimetite	$Pb_5(AsO_4)_3Cl$	–	–	–	–	✓	–
	Arsenates	Lead (II) Arsenate	$Pb_3(AsO_4)_2$	–	–	✓	–	–	–

differently from that of sulfur: the highest sulfur content (mean of 92686 $mgkg^{-1}$) is quantified in mine residues and adjacent sediments, while downstream; the concentrations in sediments decrease gradually. Hence, the contents of both elements allowed differentiation of the extent of impact represented in the sediments.

The impacted zone begins with the concentrations of sample Ss-2 adjacent to the MW-2 mine residues. The influence of the Fe—S content in the mine residues is observed in sample Ss-3, located in front of MW-1. Additionally, XRD results (Table 4) confirm that the gypsum and hydronium-jarosite contents (secondary phases) are similar for both mine residues and sample Ss-3.

Downstream, the calcium content of the samples increases significantly because of the predominant limestone geology, and the S and Fe contents remain low downstream (mean concentration of Fe = 32401 ± 6586 $mgkg^{-1}$ and S = 9296 ± 2622 $mgkg^{-1}$) due to the dilution of the material eroded from the mine residues.

4.5. Mobility tests in the San Pedro creek

The mobility test results for As, Cd, Pb and Zn from sediments and mine residues are illustrated in Fig. 4. The maximum concentrations of As from sediments Ss-3 were observed for fractions F3 (495 mgL^{-1}) and F4 (357 mgL^{-1}); this behavior indicates the association of As with iron hydroxides/oxides as an adsorbed species, and jarosite could also be an additional As source linked with these fractions.

Generally, iron oxides are considered minerals with higher thermodynamic stability than poorly crystalline iron oxyhydroxides such as ferrihydrites (Schwertmann et al., 1999) and jarosite; hence, the elements associated with the iron oxides are retained with major efficacy mainly in oxidizing environments.

Table 7
Results in comparison with previous work.

Sample	Total elemental concentrations mg kg^{-1} ($mgKg^{-1}$)					Reference
	As	Cd	Pb	Zn	Cu	
R4[a]	1637	23	17356	492	74	Vázquez (2012)
MW-2[a]	1862	36	17472	2910	126	This work
R6[b]	1752	13	37077	589	173	Vázquez (2012)
MW-1[a]	1782	31	15716	1607	131	This work

[a] Average of two samples.
[b] Average of four samples.

Table 6
Total element concentration (mean in $mgkg^{-1}$) in sediments and mine residues.

Element	LLOQ	Stream Sediments							Mine residues	
		Ss-1	Ss-2	Ss-3	Ss-4	Ss-5	Ss-6	Ss-7	MW-1	MW-2
As	15.5	39	320	1500	449	662	498	266	1782	1862
Cd	1.7	< L.L.Q.	18	66	50	27	29	23	31	36
Pb	61.3	266	1781	3908	2199	1694	2229	1382	15716	17472
Zn	15.4	180	4489	8305	4904	2769	3452	2520	1607	2910
Cu	14.7	19	79	90	87	60	70	47	131	126
Fe	15.4	19025	36766	94639	34780	32696	38836	23292	131926	112416
S	290.2	3772	4431	109095	11597	10326	9720	5542	117290	139928
Ca	50.6	98898	111459	85113	188716	204793	180669	179008	71689	68243
Mn	16.1	443	1963	976	2499	1849	2022	1397	142	403
pH	N. A.	7.46	7.85	7.17	7.85	8.04	8.14	8.34	2.55	2.69

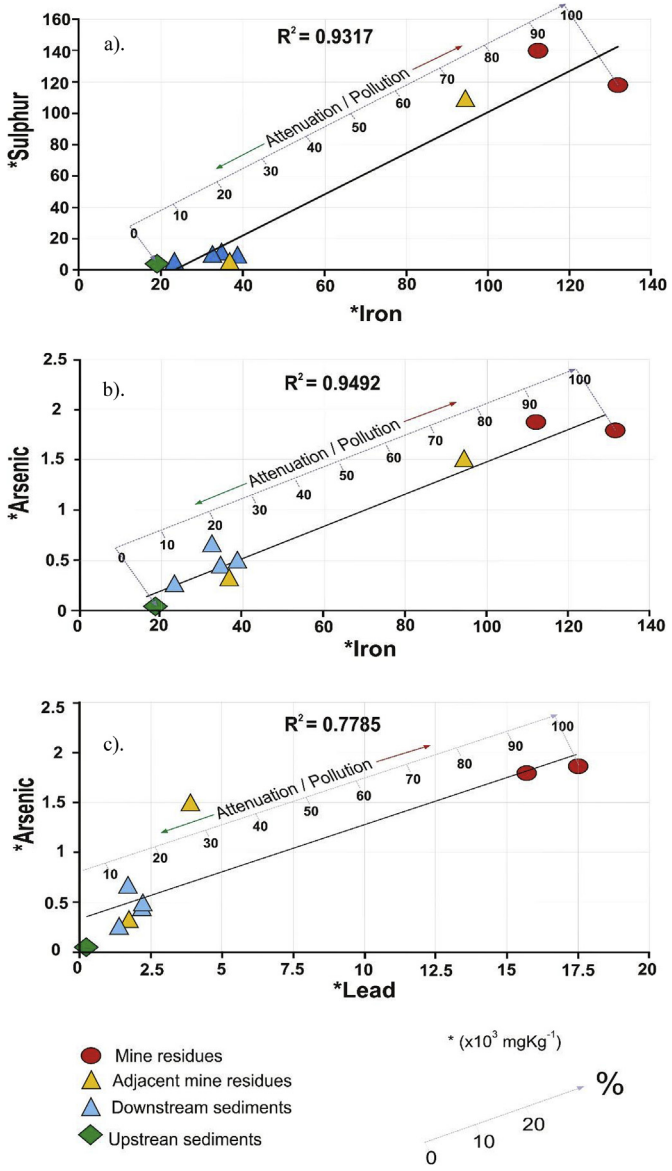

Fig. 2. Relations between; a). Fe—S, b). Fe—As and c). As—Pb in sediment and mine residue samples.

With the comparison between the iron concentrations obtained from F3 and F4, we can observe that crystalline iron oxides (F4) are more predominant than the amorphous oxyhydroxides of iron (F3), although an exception is made for Ss-1 and Ss-3: the latter includes secondary amorphous phases formed through precipitation induced by the evaporation of AMD (at circumneutral pH conditions) (Table 5). Meanwhile, the iron in mine residues for F4 (mean of 46382 ± 1078 $mgkg^{-1}$) is higher than that in mine residues for F3 (mean of 13490 ± 8 $mgkg^{-1}$), suggesting that climatic conditions (high evaporation rates and temperatures) favor the transformation of amorphous phases to crystalline iron oxides.

The presence of crystalline iron oxides in the mine residues and sediments influences the mobility and retention of the elements of environmental interest (As, Cd, Pb and Zn). Among them, several types of jarosites (i.e., hydronium jarosites, plumbojarosites) become relevant for this site, as they are highly stable under a wide range of pH (2–14) and oxidizing aerobic conditions that favor the retention of ions such as Pb^{2+} and AsO_4^{3-}.

Lead was observed mainly as plumbojarosite (Fig. 5); given that an ammonium oxalate solution can dissolve some types of jarosites (Dold, 2003), a higher concentration of this element was registered in F4 for MW-1, MW-2 and Ss-3. Although lead was also present as anglesite and cerussite, which were observed as deposits around several other particles on reactive minerals such as sulfides, given their low solubility, they seem to act as a barrier against oxidation in a phenomenon called attenuation (Lottermoser, 2007).

Since Cd and Zn present very similar geochemistry, they share comparable environmental mobility. Hence, cadmium and zinc from MW-1 and MW-2 mainly dissolve in F1 (Fig. 4 c and d), which could be related to the dissolution of nitrate and chloride salts that were formed by crystallization during evaporation processes under semiarid conditions. The major dissolution of Cd and Zn for sediments was identified in F2, which is attributed to the dissolution of sulfates (mainly Ss-3) and carbonates. In this fraction, cadmium can be released by either dissolution or desorption (Wilkie and Hering, 1996).

4.6. Mobility of PTEs and its relationship with the perched aquifer

The impact of the total content of PTEs (As, Cd, Pb and Zn) and other important elements (Ca, Fe, Mn and Sr) on the perched aquifer (cations and anions) can be directly associated with the mineralogy of both mining residues and stream sediments (Tables 4 and 5), as well as the results of the mobility tests (SSE).

Rainfall on the site generates AMD, infiltration processes along the preferential pathways (high hydraulic conductivity zones in the stream sediments and fractures) promotes dissolution of mineral phases (copiapite, goethite, coronadite and arsenolite). These reactions allow AMD neutralization and attenuation processes because of the formation of jarosites (Fig. 5) and other oxides (Tables 4 and 5); these precipitates produce suitable adsorption sites for arsenic and some of the lead. Alkaline conditions promote cadmium adsorption on particulate matter and hence decrease Cd mobility (Méndez-Ramírez and Armienta-Hernández, 2012). All of these interpretations are confirmed by the concentrations of PTEs measured in the sediments and the results of F2, F3 and F4 in SSE tests (23% As in F3 and 24% in F4; 63% Cd in F2; 18% Pb in F2, 10% in F3 and 17% in F4).

The impact of the infiltrations on the perched aquifer was monitored by means of an observation well (OW-1, Table 9). Local and intermediate groundwater flow systems along the San Pedro stream are represented in Fig. 6, the relation between the perched and the deep aquifers is also shown. Groundwater flow direction in the horizontal plane agrees with the topographic slope of San Pedro stream; it was deduced from hydraulic head measurements taken at several observation wells (not shown) in the area. The Stiff diagram for the local flow system represented by OW-1 (average composition, Table 9) indicates a $Ca—SO_4$ water type; the sulfate values are derived from reactions 1 to 3; and that of calcium, from reaction 6. Intermediate groundwater flow is represented by the composition of PW-1, in this case it is a HCO_3-Mixed water type. This composition is derived the mixture of groundwater flowing through the fractured volcanics (hydrolysis reactions including dissolution of Latite Portezuelo glassy matrix and incongruent dissolution of plagioclase) and basin fill sediments (incongruent dissolution of sanidine, Ca-montmorillonite, Na-montmorillonite and illite resulting in the formation of kaolinite, cation exchange and carbonate dissolution) included in the deep aquifer (Carrillo-Rivera et al., 2002). The predominance of silicate weathering reactions in the intermediate flow system produces higher Si values than for the local flow system. In the case of OW-1, EC values above the background values (represented by the intermediate flow system) suggest the impact of AMD infiltration and attenuation on the perched aquifer; pH measurements indicate circumneutral conditions and suggest that any infiltrating AMD was indeed neutralized. Groundwater temperature (20.5 °C) is very close to the mean summer air temperature (20 °C) because only high-intensity summer rainfall events characteristic of semiarid conditions, are able to produce natural recharge. Sulfate and calcium concentrations, as well as EC values and saturation index (Log Q/K calculated using the

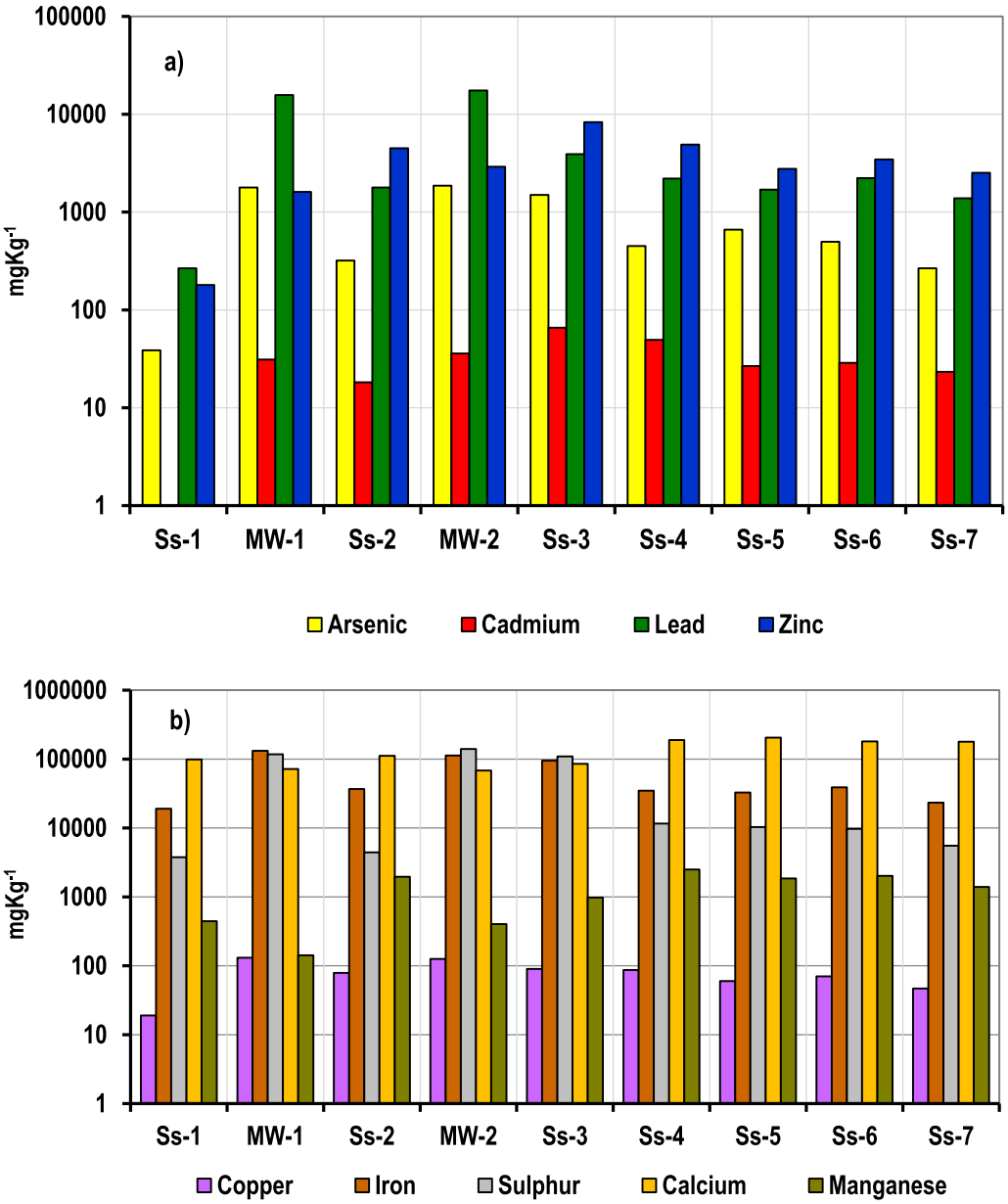

Fig. 3. Total elemental concentrations of samples: a) PTEs and b) other elements.

Geochemical Workbench software with the LLNL thermo database) for calcite (+0.315) and dolomite (+1.052), are effective indicators of attenuated AMD in natural water recharge.

In carbonate aquifers, dissolved Mg, Sr and HCO_3^- in groundwater can be used as relative residence time indicators (Edmunds et al., 1987); the measured concentrations for OW-1 are higher than those in PW-1, suggesting longer residence time, however in this case they are representing the incongruent dissolution of carbonates with AMD and

Table 8
Pearson's correlation analysis of the total elemental concentration and the pH of sediment samples.

Parameter	As	Ca	Cd	Cu	Fe	Mn	Pb	S	Zn	pH
As	1									
Ca	−0.25	1								
Cd	**0.86**	0	1							
Cu	0.65	0.05	**0.83**	1						
Fe	**0.96**	−0.47	**0.82**	0.66	1					
Mn	−0.06	0.68	0.28	0.63	−0.14	1				
Pb	**0.92**	−0.14	**0.94**	**0.86**	**0.92**	0.23	1			
S	**0.93**	−0.52	**0.78**	0.49	**0.97**	−0.33	**0.83**	1		
Zn	**0.87**	−0.26	**0.92**	**0.90**	**0.91**	0.23	**0.97**	**0.81**	1	
pH	−0.53	**0.82**	−0.34	−0.14	−0.65	0.56	−0.36	−0.72	−0.44	1

Correlation statistically significant is > 0.75.

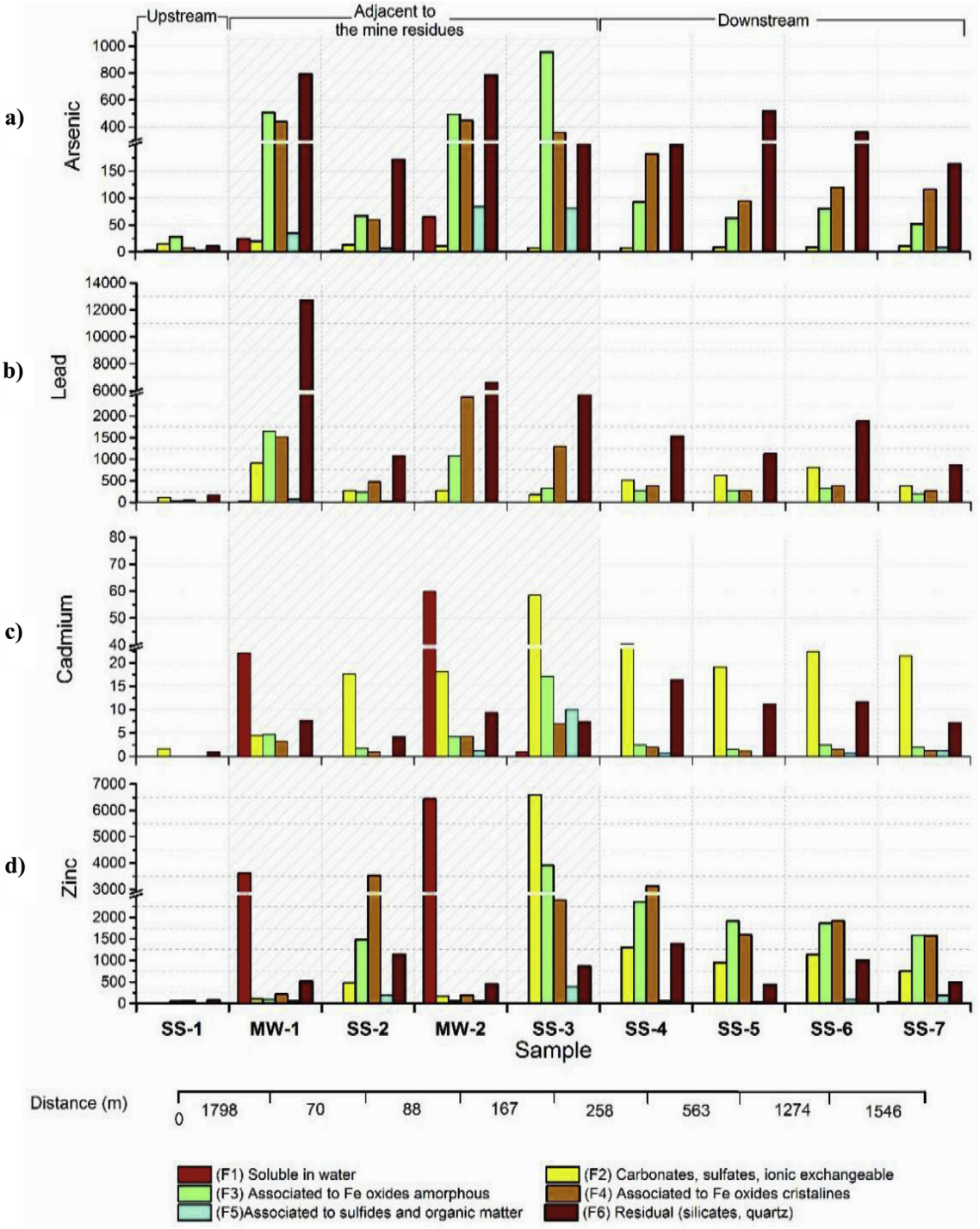

Fig. 4. Selective sequential extraction ($mgkg^{-1}$) of; a). Arsenic, b). Lead, c). Cadmium, d). Zinc (c) and distance between samples along the San Pedro stream.

represent modern recharge. This result is also supported by the low Li concentration (Table 9) and tritium values (1 ± 0.16 TU) compatible with modern recharge reported by Rivera-Armendariz (2016).

The results show that despite Sr, Mn and B show higher values than background values, the impact produced by AMD infiltration in the PTEs mobilization is limited by the attenuation processes, observed concentrations for PTE's are below international drinking water standards (USEPA, 2009; WHO, 2011). Adsorption processes in the vadose zone seem to be very efficient for attenuation of As and Cd; aerobic (DO ≈ 3–4 mg/l) and oxidizing (Eh ≈ 350 mV) conditions favor the stability of goethite (saturation index of 5.05, low dissolved Fe concentration), which are additional factors contributing to the stabilization of As. The higher As concentration for PW-1 is linked to interaction with the geogenic primary sources in the fractured volcanic rocks (mainly the glassy matrix), in addition to residence time and circulation depth (Banning, 2012), as evidenced by the water temperature and water type. Although Pb and Zn concentrations are below drinking water standards, the values show further evidence of the AMD impact on the perched aquifer; even though the concentrations of these elements could be higher, the saturation index values (cerussite −4.28 and smithsonite −2.15) show they are subsaturated. Because of the semiarid conditions, only a few rainfall events can produce natural recharge and therefore possible conditions for groundwater impact due to AMD infiltration. This situation explains why a higher impact is

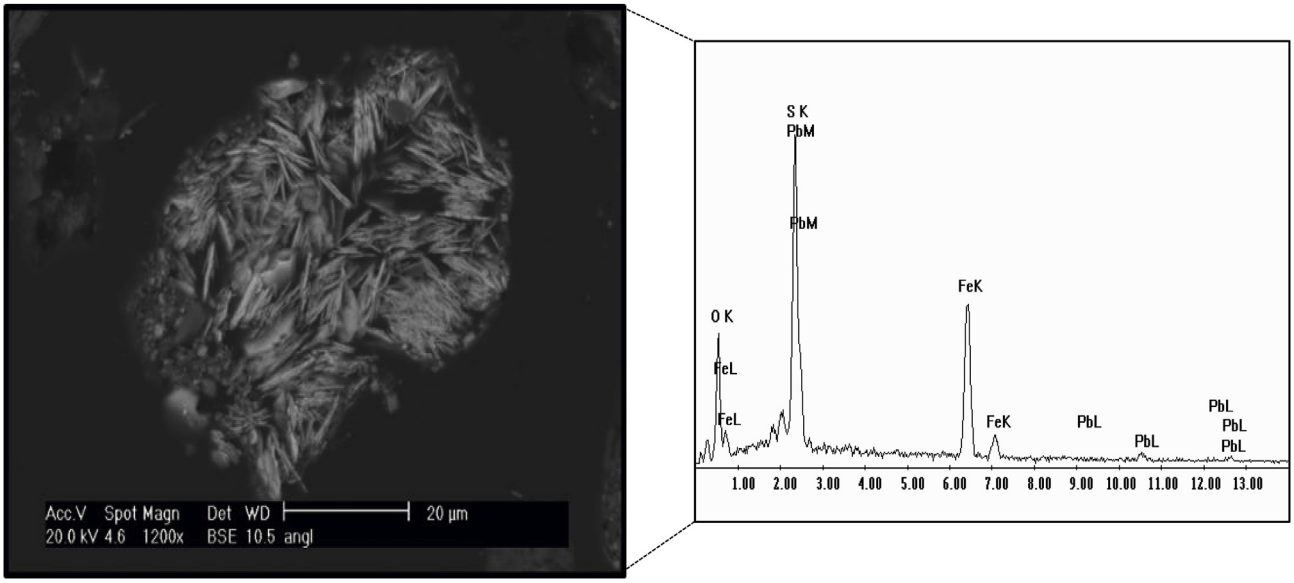

Fig. 5. SEM image and the microanalysis spectrum of a particle of plumbojarosite ($Pb_{0.5}Fe_3(SO_4)_2(OH)_6$).

observed on sediments than on groundwater.

5. Conclusions

This study shows the impact of ancient mine residues on sediments downstream from an ancient dumping site along 5.764 km of an ephemeral stream under semiarid conditions. The primary source for contaminants is an ancient mine residue pile that contains primary (sulfides, calcite and quartz) and secondary (sulfates and oxides) phases that generate AMD under weathering conditions.

A mineralogical characterization showed that carbonates, sulfates and sulfides were the main mineral phases in the sediments, and minor

Table 9
Average of field parameters and geochemical analyses for OW-1 and PW-1.

Data	Parameters	Units	OW-1	PW-1	MCL[a]	Reference
Aquifer	—	—	Perched	Deep	—	—
—	Period	Year	2014–2016	2013–2016	—	—
Field measurements	n	—	5	10	—	—
	pH	—	7.16	7.69	6.5–8.5	WHO
	Temperature	°C	20.48	30.84	—	—
	EC	µS/cm	1302.00	306.17	—	—
	TDS	mgL^{-1}	754.20	165.35	1000	WHO
	Eh	mV	391.88	337.17	—	—
	DO	mgL^{-1}	4.01	3.33	—	—
	Total alkalinity	mgL^{-1}	219.70	104.80	—	—
	Total hardness	$CaCO_3$	650.29	75.34	500	WHO
Cations	Ca^{2+}	mgL^{-1}	210.74	26.95	—	—
	Na^{2+}	mgL^{-1}	38.56	25.77	200	WHO
	K^{+}	mgL^{-1}	3.29	7.09	—	—
	Mg^{2+}	mgL^{-1}	41.12	1.90	—	—
Anions	SO_4^{2-}	mgL^{-1}	536.30	7.67	400	—
	HCO_3^{-}	mgL^{-1}	228.44	136.27	—	—
	$N{-}NO_3^{-}$	mgL^{-1}	5.08	2.48	10	USEPA
	Cl^{-}	mgL^{-1}	26.75	15.32	250	WHO
	F^{-}	mgL^{-1}	0.37	0.58	1.5	WHO
PTEs	As	μgL^{-1}	2.45	10.17	10	WHO
	Cd	μgL^{-1}	< 0.014	0.06	3	WHO
	Pb	μgL^{-1}	2.66	0.46	10	WHO
	Zn	μgL^{-1}	65.33	4.36	3000	WHO
Colloids and trace elements	Si	mgL^{-1}	25.07	32.48	—	—
	Fe	μgL^{-1}	17.64	32.97	300	WHO
	Li	μgL^{-1}	4.74	34.86	—	—
	B	mgL^{-1}	0.09	0.05	0.5	WHO
	Mn	μgL^{-1}	19.13	0.62	400	WHO
	Sr	μgL^{-1}	1402.08	108.55	—	—

[a] MCL: Maximum contaminant level, WHO (2011), USEPA (2009).

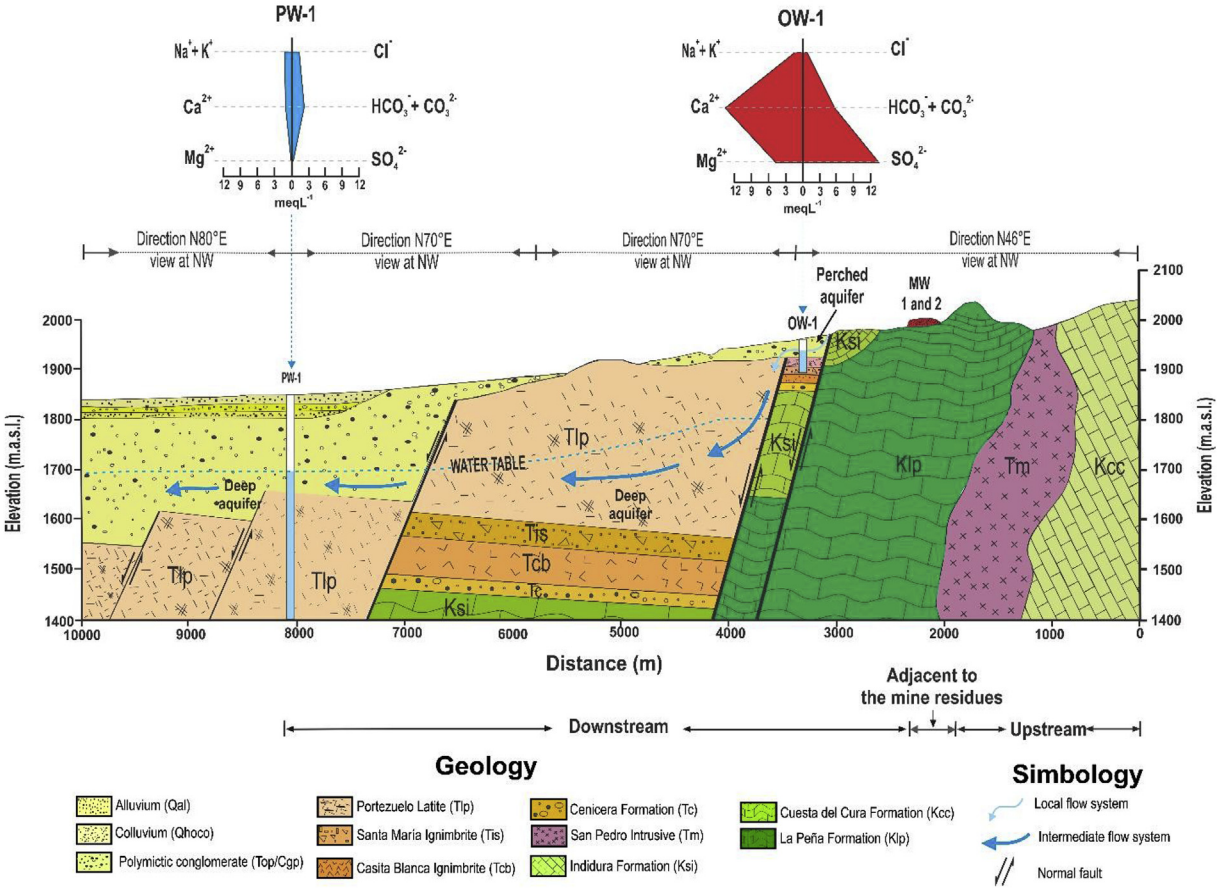

Fig. 6. Geological section along the San Pedro stream depicting aquifers and groundwater quality.

amounts of silicates and oxides were also identified. The environmental importance of the mineralogy of the site was confirmed. The total concentrations of As, Cd, Pb and Zn were used as indicators of the impact of the mine residue dispersion on the sediments. Zn and Pb presented the highest concentrations, which correlated with the content of sulfide particles and the content of these elements in secondary phases (carbonates and sulfates) produced mainly by AMD reactions in the stream sediments. The total As and Cd concentrations were lower than those of Pb and Zn; however, the former were up to 15–20 times higher than the background values. SSE tests showed that Cd and Zn have the highest mobilities, the former particularly from the dissolution of carbonates and sulfates as well as ion exchange reactions, and the latter also from oxides. Although SSE tests are useful to determine the potential mobilization of elements, particularly PTEs, in this case, it was shown that these tests were not definitive to establish environmental impacts on water. The natural recharge impacted by AMD, as identified in the perched aquifer, indicated that high sulfate concentration and hardness (both above drinking water standards) were produced by AMD attenuation reactions in the vadose zone, and then these species could be mobilized to the groundwater environment; however, the concentrations of relevant PTEs such as As and Cd, were below background values, which was an indication of the effective attenuation in the vadose zone. Lead and Zn concentrations were below drinking water international standards; however, their concentrations were higher than the background concentrations, which further confirmed the contribution of AMD to natural recharge. The results are an important example of the impact of ancient mining residues on the dispersion of contaminants in a semiarid environment, as shown by the PTE concentrations in sediments, and an example of the effective attenuation processes that prevented groundwater contamination. Because of the semiarid conditions, only a few rainfall events produce natural recharge and therefore the possible conditions for groundwater impact due to AMD infiltration. This situation explains why a higher impact is observed on sediments than on groundwater.

Considering that similar sites with sulfide mining operations under semiarid conditions with the presence of limestones are found along the Sierra Madre Oriental, the results of this study can be useful in understanding the mobility of PTEs in sediments and water.

Acknowledgements

The authors are thankful for the support of G. Aragón to obtain SEM images, M.E. García, M.G. Hernandez and M. Cortina for chemical analyses performed at the Water and soil chemistry laboratory of the Engineering Faculty-Geology Institute-UASLP; R. Tovar for XRD analyses and C. A. Rivera and S. Alonso for elaboration of Fig. 6. This work was financially supported by the National Council of Science and Technology (CONACyT) through grant FORDECyT 190966. Montes-Ávila thanks CONACyT for scholarship number 349150.

References

Al, T.A., Martin, C.J., Blowes, D.W., 2000. Carbonate-mineral/water interactions in sulfide-rich mine tailings. Geochem. Cosmochim. Acta 64 (23), 3933–3948. https://doi.org/10.1016/S0016-7037(00)00483-X.

Alloway, B.J., 1995. The origins of heavy metals in soils. In: Alloway, B.J. (Ed.), Heavy Metals in Soil, second ed. Blackie Academic and Professional, London, Eng, pp. 38–55 ISBN 0-7514-0198-6.

Árcega-Cabrera, F., Castillo-Blum, S.E., Armienta, H.,M.A., 2005. Kinetic study of the release of lead in a mine-impacted tropical river. Bull. Environ. Contam. Toxicol. 75, 523–529. https://doi.org/10.1007/s00128-005-0783-z.

Banning, A., Cardona, A., Rüde, T.R., 2012. Uranium and arsenic dynamics in volcano-

sedimentary basins–An exemplary study in North-Central Mexico. Appl. Geochem. 27 (11), 2160–2172. https://doi/10.1016/j.apgeochem.2012.01.001.
Berner, R.A., 1978. Rate control of mineral dissolution under earth surface conditions. Am. J. Sci. 278 (9), 1235–1252. https://doi/10.2475/ajs.278.9.1235.
Brown Jr., G.E., Calas, G., Hemley, R.J., 2006. Scientific advances made possible by user facilities. Elements 2, 23–30. https://doi.org/10.2113/gselements.2.1.9.
Burdon, D.J., 1998. Semiarid regions. In: Encycolopedia of Hydrology and Lakes. Part 18. Encyclopedia of Earth Science. Springer Netherlands, pp. 601–607.
Cardona, A., Banning, A., Carrillo-Rivera, J.J., Aguillón-Robles, A., Rüde, T.R., Aceves-de-Alba, J., 2018. Natural controls validation for handling elevated fluoride concentrations in extraction activated Tóthian groundwater flow systems: San Luis Potosí, Mexico. Environ. Earth Sci. 77 (121), 1–13. https://doi.org/10.1007/s12665-018-7273-1.
Carrillo-Chávez, A., Morton-Bermea, O., González-Partida, E., Rivas-Solórzano, H., Oesler, G., García-Meza, V., Hernández, E., Morales, P., Cienfuegos, E., 2003. Environmental geochemistry of the Guanajuato mining district, Mexico. Ore Geol. Rev. 23 (Issues 3–4), 277–297. https://doi/10.1016/S0169-1368(03)00039-8.
Carrillo-Chávez, A., Salas-Megchún, E., Levresse, G., Muñoz-Torres, C., Pérez-Arvizu, O., Gerke, T., 2014. Geochemistry and mineralogy of mine-waste material from a "skarn-type" deposit in central Mexico: modeling geochemical controls of metals in the surface environment. J. Geochem. Explor. 144, 28–36. https://doi.org/10.1016/j.gexplo.2014.03.017.
Carrillo-Rivera, J.J., Cardona, A., Edmunds, W.M., 2002. Use of abstraction regime and knowledge of hydrogeological conditions to control high-fluoride concentration in abstracted groundwater: San Luis Potosí basin. México. 2002 J. Hydrol. 261, 24–47. https://doi.org/10.1016/S0022-1694(01)00566-2.
Castro-Larragoitia, J., Kramar, U., Puchelt, H., 1997. 200 years of mining activities at La Paz/San Luis Potosí/Mexico–Consequences to environment and geochemical exploration. J. Geochem. Explor. 58, 81–91. https://doi.org/10.1016/S0375-6742(96)00054-4.
Castro-Larragoitia, J., Kramar, U., Monroy-Fernández, M.G., Viera-Décida, F., García-González, E.G., 2013. Heavy metal and arsenic dispersion in a copper-skarn mining district in a Mexican semi-arid environment: sources, pathways and fate. Environ. Earth Sci. 69, 1915–1929. https://doi.org/10.1007/s12665-012-2024-1.
CEM, 2015a. Application note for acid digestion. SW846-3052 - soil and sediment total digestion. Consulted in: http://www.cem.com/download156.html .
CEM, 2015b. Application note for acid digestion. Boric acid neutralization. Consulted in. http://www.cem.com/download156.html.
COREMI, 1996. Geological-mining Monograph of the State of San Luis Potosí, second ed. Consejo de Recursos Minerales. Secretaría de Comercio y Fomento Industrial, Pachuca, Hidalgo, México, pp. 62–66.
Cornell, R.M., Schwertmann, U., 2003. The Iron Oxides. Structure, Properties, Reactions, Occurrences and Uses, vol. 664 Wiley-VHC.Weinheim ISBN 3-527-30274-3.
Dold, B., 2003. Speciation of the most soluble phases in a sequential extraction procedure adapted for geochemical studies of copper sulfide mine waste. J. Geochem. Explor. 80, 55–68. https://doi.org/10.1016/S0375-6742 (03)00182-1.
Dold, B., Fontboté, L., 2001. Element cycling and secondary mineralogy in porphyry copper tailings as a function of climate, primary mineralogy, and mineral processing. J. Geochem. Explor. 74 (1–3), 3–55.
Dold, B., Wade, Ch, Fontboté, Ll, 2009. Water management for acid mine drainage control at the polymetallic Zn-Pb-(Ag-Bi-Cu) deposit Cerro de Pasco, Peru. J. Geochem. Explor. 100, 133–141. https://doi.org/10.1016/j.gexplo.2008.05.002.
Eaton, A.D., Clesceri, L.S., Rice, E.W., Greenberg, A.E., 2005. Standard Methods for the Examination of Water and Wastewater, 21st ed. APHA American Public Health Association, Washington, DC.
Edmunds, W.M., Cook, J.M., Darling, W.G., Kinniburgh, D.G., Miles, D.L., Bath, A.H., Andrews, J.N., 1987. Baseline geochemical conditions in the Chalk aquifer, Berkshire, UK: a basis for groundwater quality management. Appl. Geochem. 2 (3), 251–274.
Espejo, L., Kretschmer, N., Oyarzún, J., Meza, F., Núñez, J., Maturana, H., Soto, G., Oyarzo, P., Garrido, M., Suckel, F., Amezaga, J., Oyarzún, R., 2012. Application of water quality indices and analysis of the surface water quality monitoring network in semiarid North-Central Chile. Environ. Monit. Assess. 184, 5571–5588. https://doi.org/10.1007/s10661-011-2363-5.
Espinosa, E., Armienta, M.A., Cruz, O., Aguayo, A., Ceniceros, N., 2009. Geochemical distribution of arsenic, cadmium, lead and zinc in river sediments affected by tailings in Zimapán, a historical polymetallic mining zone of México. Environ. Geol. 58, 1467–1477. https://doi.org/10.1007/s00254-008-1649-6.
García-Lorenzo, M.L., Pérez-Sirvent, C., Martínez-Sánchez, M.J., Molina-Ruiz, J., 2012. Trace elements contamination in an abandoned mining site in a semiarid zone. J. Geochem. Explor. 113, 23–35. https://doi.org/10.1016/j.gexplo.2011.07.001.
Gómez-Álvarez, A., Valenzuela-García, J.L., Meza-Figueroa, D., de la O-Villanueva, M., Ramírez-Hernández, J., Almendariz-Tapia, J., Pérez-Segura, E., 2011. Impact of mining activities on sediments in a semi-arid environment: San Pedro River, Sonora, Mexico. Appl. Geochem. 26, 2101–2112. https://doi.org/10.1016/j.apgeochem.2011.07.008.
Hayes, S.M., Webb, S.M., Bargar, J.R., O´Day, P.A., Maier, R.M., Chorover, J., 2012. Geochemical weathering increases lead bioaccessibility in semi-arid mine tailings. Environ. Sci. Technol. 46, 5834–5841. https://doi.org/10.1021/es300603s.
Hudson-Edwards, K.A., Jamieson, H.E., Charnock, J.M., Mackling, M.G., 2005. Arsenic speciation in waters and sediment of ephemeral floodplain pools, Ríos Agrio-Guadiamar, Aznalcóllar, Spain. Chem. Geol. 219, 175–192. https://doi.org/10.1016/j.chemgeo.2005.02.001.
Labarthe-Hernández, G., Tristán-González, M., Aranda-Gómez, J.J., 1982. Revisión estratigráfica del Cenozoico de la parte central del estado de San Luis Potosí: universidad Autónoma de San Luis Potosí. Instituto de Geología y Metalurgia, Folleto Técnico 85 (208), 1.
Lindsay, M.B.J., Moncur, M.C., Bain, J.G., Jambor, J.L., Ptacek, C.J., Davies, D.W., 2015. Geochemical and mineralogical aspects of sulphide mine tailings. Appl. Geochem. 57, 157–177. https://doi.org/10.1016/j.apgeochem.2015.01.009.
López-Doncel, R., 2003. La Formación Tamabra del Cretácico medio en la porción central del margen Occidental de la Plataforma Valles-San Luis Potosí, centro-noreste de México. Rev. Mex. Ciencias Geol. 20 (1), 1026–8774.
Lottermoser, B., 2007. Mine Wastes: Characterization, Treatment and Environmental Impacts, second ed. Springer-Verlag, Berlin, pp. 400. https://doi.org/10.1007/978-3-642-12419-8.
Maher, K., 2010. The dependence of chemical weathering rates on fluid residence time. Earth Planet Sci. Lett. 294, 101–110. https://doi.org/10.1016/j.epsl.2010.03.010.
Martínez Chavez, P.A., 2012. Historia ambiental del municipio de cerro de San Pedro, San Luis Potosí, México (Siglo XX). Tesis doctoral. Programas Multidisciplinarios de Posgrado en Ciencias Ambientales. Universidad Autónoma de San Luis Potosí, San Luis Potosí, México 289 pp. Consulted in: http://ninive.uaslp.mx/jspui/handle/i/3706.
Méndez-Ramírez, M., Armienta-Hernández, M.A., 2012. Distribución de Fe, Zn, Pb, Cu, Cd y As originada por residuos mineros y aguas residuales en un transecto del Río Taxco en Guerrero, México. Rev. Mex. Ciencias Geol. 29 (2), 450–462.
Navarro, M.C., Pérez-Sirvent, C., Martínez-Sánchez, M.J., Vidal, J., Tovar, P.J., Bech, J., 2008. Abandoned mine sites as a source of contamination by heavy metals: a case study in a semi-arid zone. J. Geochem. Explor. 96. https://doi.org/10.1016/j.gexplo.2007.04.011.
Plant, J.A., Hale, M., 1994. Introduction: the foundations of modern drainage. In: In: Plant, J.A., Hale, M. (Eds.), Drainage Geochemistry, vol. 6. Elsevier Science, pp. 3–9. Handbook of Exploration Geochemistry. https://doi.org/10.1016/B978-0-444-81854-6.50007-9.
Plumlee, G.S., 1999. The environmental geology on mineral deposits. In: In: Plumlee, G.S., Logsdon, M.J. (Eds.), The Environmental Geochemistry of Mineral Deposits. Part A: Processes, Techniques and Health Issues, vol. 6A. Society of Economic Geology, Inc. Littleton, Col., USA, pp. 71–114 Reviews in Economic Geology.
Ramos-Arroyo, Y.R., Prol-Ledesma, R.M., Siebe-Grabach, C., 2004. Características geológicas y mineralógicas e historia de extracción del distrito de Guanajuato, México. Posibles escenarios geoquímicos para los residuos mineros. Rev. Mex. Ciencias Geol. 21 (2), 268–284 ISSN 1026-8774.
Razo, I., Carrizales, L., Castro, J., Díaz-Barriga, F., Monroy, M., 2004. Arsenic and heavy metal pollution of soil,water and sediments in a semi-arid climate mining area in Mexico. Water. Air and Soil pollution 152, 129–152. https://doi.org/10.1023/B:WATE.0000015350.14520.c1.
Razo, S.,I., Muñoz, G.,R., Cepeda, B.,C., Monroy, F.M., 2007. Caracterización ambiental de residuos mineros históricos del distrito minero Cerro de San Pedro (San Luis Potosí, México). Memoria Convención minera AIMMGM 352–357. Tomo 1, No 27. http://www.sgm.gob.mx/aimmgm/JspInforme.jsp.
Ribeiro de Souza, L., Knöller, K., Queiroz Ladeira, A.C., 2016. Sulfur isotope fractionation and sequential extraction to assess metal contamination on lake and river sediments. J. Soils Sediments 16, 1986–1994. https://doi.org/10.1007/s11368-016-1410-9.
Rivera-Armendáriz, C.H., 2016. "Geoquímica y datación de sistemas de flujo de aguas subterránea: cuencas de San Luis Potosí, Matehuala y Lagunas de Mayran Viesca y Sierra de Rodríguez". Tesis Maestría en Geología Aplicada. Posgrado en Geología Aplicada. Universidad Autónoma de San Luis Potosí, San Luis Potosí, México, pp. 151.
Rodríguez Torres, P., 2013. Evaluación fisiológica de especies vegetales que crecen en sitios impactados por residuos generadores de drenaje ácido de roca. Tesis Maestría en Ciencias Ambientales. Programas Multidisciplinarios de Posgrado en Ciencias Ambientales. Universidad Autónoma de San Luis Potosí, San Luis Potosí, México 232 pp. Consulted in: http://comunidadpmpca.uaslp.mx/tesis.aspx.
Rodríguez-Rodríguez, Y., 2011. Evaluación de la contaminación por metales en pasivos ambientales de actividades metalúrgicas históricas en el distrito minero Cerro de San Pedro, S. L. P. (México). Tesis de Maestría en Ciencias Ambientales. Programas Multidisciplinarios de Posgrado en Ciencias Ambientales. Universidad Autónoma de San Luis Potosí, San Luis Potosí, México, pp. 161. http://comunidadpmpca.uaslp.mx/tesis.aspx.
Salomons, W., 1995. Environmental impact of metals derived from mining activities: processes, predictions, prevention. J. Geochem. Explor. 52, 5–23. https://doi.org/10.1016/0375-6742(94)00039-E.
Salomons, W., 1998. Biogeodynamics of contaminated sediments and soils: perspectives and future research. J. Geochem. Explor. 62, 37–40. https://doi.org/10.1016/S0375-6742(97)00063-0.
Schaider, L.A., Senn, D.B., Estes, E.R., Brabander, D.J., Shine, J.P., 2014. Sources and fates of heavy metals in a mining-impacted stream: temporal variability and the role of iron oxides. Sci. Total Environ. 490, 456–466. https://doi.org/10.1016/j.scitotenv.2014.04.126.
Schwertmann, U., Friedl, J., Stanjek, H., 1999. From Fe(III) ions to ferrihydrite and then to Hematite. J. Colloid Interface Sci. 209, 215–223. https://doi.org/10.1006/jcis.1998.5899.
Shang, Ch, Zelazny, L.W., 2008. Selective dissolution techniques for mineral analysis of soils and sediments. In: Methods of Soil Analysis. Part 5. Mineralogical Methods. SSSA Book Series. Soil Science Society of America. Segoe Road, Madison, WI, U.S.A, pp. 33–80.
Smith, K.S., Huyck, H.L.O., 1999. An overview of the abundance, relative mobility, bioavailability, and human toxicity of metals. In: Plumlee, G.S., Logsdon, M.J. (Eds.), The Environmental Geochemistry of Mineral Deposits. Part A: Processes, Techniques and Health Issues. vol. 6A. Society of Economic Geology, Inc., Littleton, Col., USA, pp. 29–70 Reviews in Economic Geology ISSN 0741–0123.
SMN, 2015. Normales climatológicas, Estación 00024111, san Luis Potosí, san Luis Potosí

(SMN), periodo 1951-2000. Servicio meteorológico Nacional. Consulted in: http://smn.cna.gob.mx/index.php?option=com_content&view=article&id=172&tmpl=component.

Talavera, M.O., Armienta, H.M.A., García, A.J., Flores, M.N., 2006. Geochemistry of leachates from the El Fraile sulfide tailings pile in Taxco, Guerrero, southern Mexico. Environ. Geochem. Health 28, 243–255. https://doi.org/10.1007/s10653-005-9037-6.

Tessier, A., Campbell, P.G., Bisson, M., 1979. Sequential extraction procedure for the speciation of particulate trace metals. Anal. Chem. 51 (7), 844–851 ISSN 0003-2700.

Ure, A.M., Davidson, C.M., 2002. Introduction. In: Ure, A.M., Davidson, C.M. (Eds.), Chemical Speciation in the Environment, second ed. pp. 1–5. Blackwell Science. https://doi.org/10.1002/9780470988312.ch10.

USEPA, 1996. Method 3052. Microwave Assisted Acid Digestion of Siliceous and Organically Based Matrices. United States Environmental Protection Agency, pp. 20. Available online. https://www.epa.gov/hw-sw846/sw-846-test-method-3052-microwave-assisted-acid-digestion-siliceous-and-organically-based, Accessed date: 17 January 2018.

USEPA, 2004. Method 9045D. Soil and Waste PH. United States Environmental Protection Agency, pp. 5. Available online at: https://www.epa.gov/dwstandardsregulations, Accessed date: 10 February 2018.

USEPA, 2009. Ground water and drinking water. National primary drinking water regulation table. Available online at: https://www.epa.gov/dwstandardsregulations, Accessed date: 10 February 2018.

USEPA, 2014. Method 6010D. Inductively Coupled Plasma-optical Emission Spectrometry. SW-846 Update V. United States Environmental Protection Agency, pp. 35. Available online at: https://www.epa.gov/sites/production/files/2015-12/documents/6010d.pdf, Accessed date: 10 February 2018.

Vázquez, V.S.E., 2012. Caracterización de un depósito no controlado de residuos mineros y evaluación de su impacto en suelo superficial. Tesis Maestría en Geología Aplicada. Posgrado en Geología Aplicada. Universidad Autónoma de San Luis Potosí, San Luis Potosí, México 131 pp.

WHO, 2011. WHO Guidelines for Drinking Water Quality Geneva, fourth ed. . Available online at: http://www.who.int , Accessed date: 10 February 2018.

Wilkie, J.A., Hering, J.G., 1996. Adsorption of arsenic onto hydrous ferric oxide: effects of adsorbate/adsorbent ratios and co-occurring solutes. Colloid. Surface. Physicochem. Eng. Aspect. 107, 97–110. https://doi.org/10.1016/0927-7757(95)03368-8.

Zhu, M., Legg, B., Zhang, H., Gilbert, B., Ren, Y., Banfield, J.F., Waychunas, G.A., 2012. Early stage formation of iron oxyhydroxides during neutralization of simulated acid mine drainage solutions. Environ. Sci. Technol. 46, 8140–8147. https://doi.org/10.1021/es301268g.